Measuring 2012 Photon Trigger Efficiency in the ATLAS Experiment

David Layden

Honours Mathematical Physics
University of Waterloo

Completed under the supervision of:

Brigitte Vachon

Department of Physics
McGill University

August 22, 2013

Acknowledgements

I would like to thank the Institute of Particle Physics (IPP) for providing me with the incredible opportunity to participate in CERN's summer student program. I am also grateful to the entire McGill ATLAS group for their warm welcome and constant support throughout the term. I am particularly obliged to Robert Keyes, Sébastien Prince, Benoit Lefebvre and Mark Stockton for volunteering their expertise, and to François Corriveau for his help, guidance and unofficial supervision. Finally, this work would not have been possible if it weren't for the direction and technical know-how of Michael Stoebe, as well as the vision and constant support of my supervisor Brigitte Vachon, to whom I am greatly indebted.

This work was supported in part by the Natural Sciences and Engineering Research Council of Canada (NSERC).

Contents

List of Figures

Summary

In this report I present my work on ATLAS photon trigger efficiency, completed in the summer of 2013 at McGill University and CERN, as part of the latter's summer student program.

The measurement of differential inclusive photon production cross section represents a direct test of the Standard Model, and when computed with 2012 ATLAS data, it is a direct test in a new energy regime. In order to measure this cross section, one must first measure the efficiency of the photon triggers used to collect the relevant data. Of particular interest, is the efficiency of the trigger chain *g20_loose*, as the efficiencies of chains with higher energy cutoffs are measured with respect to it.

Under the supervision of Brigitte Vachon, and with the help of her graduate student Michael Stoebe, I measured the efficiency of *g20_loose* in 2012 with respect to offline tight leading photons. To do so, I employed the bootstrap method to decompose the efficiency of the chain, in order to reduce uncertainties.

I found the aforementioned trigger to be within 1% of full efficiency for values of photon transverse energy greater than 23 GeV. Due to the rapidly falling energy spectrum of tight leading photons, and the relatively small size of the minimum bias sample used in this study, the uncertainties on the *g20_loose* efficiency are somewhat large in the high E_T^γ region. If this proves to be a limiting factor in the inclusive photon cross section measurement, we may complement this work with a radiative Z decay analysis.

1 Introduction

The Standard Model of particle physics is the current mainstream theory of fundamental particles and their interactions. It has been extremely successful since its development in the early 1970s, and has managed to explain *most* experimentally observed phenomena with incredible precision. However, the Standard Model does not give us the whole picture: it does not incorporate gravity, nor does it provide any answers as to the nature of dark matter, or the huge excess of matter compared to antimatter in our universe [1]. Thus, while the Standard Model represents the extent of our current understanding of particle physics, we know that it cannot continue to hold indefinitely, and so it is essential to push its limits experimentally to see how far it can take us, and what the next generation of theories should look like.

The Large Hadron Collider (LHC) is the world's largest and highest energy particle accelerator, capable of accelerating protons to nearly the speed of light in opposing directions before colliding them. Such collisions result in an almost inconceivably large energy density in the vicinity of the protons, allowing for the creation of a great number of fundamental particles which are not observed at more familiar energy scales. These collisions—which provide an excellent testing ground for the Standard Model—are made to occur inside one of four main detectors, which record the resulting outpouring of particles.

One such detector, the ATLAS[1] experiment, is a 7000 ton toroidal instrument constructed around the collision point, which records and identifies the particles resulting from proton-proton collisions. It is a general-purpose detector, designed to be sensitive to many types of new physics, including electroweak symmetry breaking, supersymmetry, extra dimensions, new heavy gauge bosons etc. [2]. It is not hard to imagine that such an ambitiously designed apparatus would have to address a long series of experimental challenges. One such challenge comes from the fact that protons are not accelerated one at a time, but rather in bunches of $\sim 10^9$, and so collisions occur at a rate which is unmanageably high as far as data acquisition (DAQ) is concerned. However, most of these collision events involve protons deflecting off of one-another, rather than "head-on" collisions, and thus are not particularly interesting for our current studies. Thus, to reduce the data rate, the ATLAS experiment uses a sophisticated trigger system which decides in real time which events are potentially interesting, and which ones can be ignored.

One type of particularly interesting event is that in which at least one photon is produced directly from the initial collision (denoted $pp \to \gamma + X$), as opposed to being produced uniquely in the messy aftermath in the detector. The results obtained by studying such collisions comprise a direct test of the Standard Model, and can also be sensitive to new physics, should discrepancies between theory and experiment be observed [3]. However, in order to obtain such results, it is crucial that one quantify how the trigger system behaved during data-

[1] ATLAS is an acronym for "A Toroidal LHC Apparatus"

taking, a task around which my work has been centred.

In this report I will present the work I have completed while in the ATLAS group at McGill and at CERN, under the supervision of Prof. Brigitte Vachon, in collaboration with Michael Stoebe and Dr. Mark Stockton.

2 Inclusive Photon Cross Section

Conceptually, the term inclusive photon cross section (or inclusive photon production cross section) refers to the probability of one or more photons being produced by a collision. Usually, we are interested in how this cross section relates to some kinematic variable, such as the transverse energy[2] of the leading photon.

2.1 Cross Section

The term *cross section* comes from the early days of particle physics, in which particles were thought of like small marbles. When two marbles are rolled towards each other, the probability of a collision is proportional to their sizes; in other words, bigger marbles are more likely to collide. This way of picturing particle collisions is incorrect, but the idea of cross section has become the *de facto* measure of the probability of a certain reaction occurring. The problem is, particles are fundamentally unlike marbles; rather, they are quantum clouds of probability which interact with each other in complex ways. For example, if two particles are attracted to one another (say through electromagnetic interaction), they are much more likely to collide, and thus their cross sections are larger than their physical "sizes". Despite these conceptual complications, cross sections are ubiquitous in particle physics, and they have the distinct advantage of allowing for the direct comparison of results between different accelerators [4].

Suppose that N denotes the number of occurrences of a certain collision outcome, then the rate at which the events occur in the ATLAS detector is given by

$$\frac{dN}{dt} = \mathcal{L}\sigma, \tag{1}$$

where σ is the cross section of the reaction and $\mathcal{L} = \mathcal{L}(t)$ is the instantaneous luminosity, a measurable characteristic of the proton beam. Cross sections have units of area (usually measured in *barns*, denoted b), thus $\mathcal{L}$ has units of area

[2]Transverse energy, denoted E_T, refers to the component of a particle's energy associated with movement orthogonal to the beam axis. For photons, the transverse momentum p_T, defined in an analogous way, is equal to the transverse energy, and the two can be used interchangeably.

per time. Integrating both sides of Eq. (1) with respect to time, one finds that

$$N = \sigma \underbrace{\int dt\, \mathcal{L}}_{L} = \sigma L, \tag{2}$$

as σ is, of course, time-invariant. Here, L is the integrated luminosity of the beam over a given time period, and has units of inverse area. The integrated luminosity of the 2012 ATLAS data, for example, was of 21.7 fb^{-1}, which is a measure of the number of collisions observed.

2.2 Inclusive Photon Production

As previously mentioned, inclusive photon production refers to events in which at least one photon is produced from the pp collision. Such events are important for t quark and W mass measurements, and can be sensitive to new physics, as exemplified in Fig. (1) [5]. The differential cross section of inclusive photon production ($d\sigma/dE_T^\gamma$) provides a direct test of Standard Model predictions, and with the unprecedented centre of mass energy of the 2012 LHC run, it will provide such a test in a new energy regime.

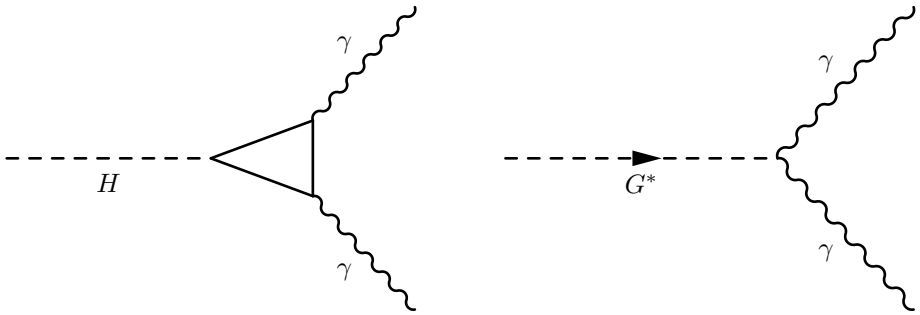

(a) $H \to \gamma\gamma$ (b) $G^* \to \gamma\gamma$

Figure 1: Photon-producing events can be sensitive to new physics: Panel (a) depicts one of the main channels involved in the discovery of the Higgs boson, while Panel (b) shows a hypothetical graviton decay mode.

However, in order to compute the differential inclusive photon production cross section, it is essential that one first quantify the performance of the photon trigger chains used in the data taking. More specifically, one must measure the efficiency of the triggers with respect to offline-identified photons.

3 ATLAS Trigger System

The ATLAS experiment is a general-purpose detector designed to be sensitive to a wide range of new physics. While it has already produced many interesting results, its operation is continuously subject to a variety of experimental challenges, notably that of reducing the enormous amount of raw data that is initially produced.

3.1 The ATLAS Detector

A schematic of the detector is shown in Fig. (2), where one can see the various layered components of the detector. The particles produced from pp collisions in the centre are ejected from collision site and enter the detector, where they interact in different ways with the various layers depending on their type.

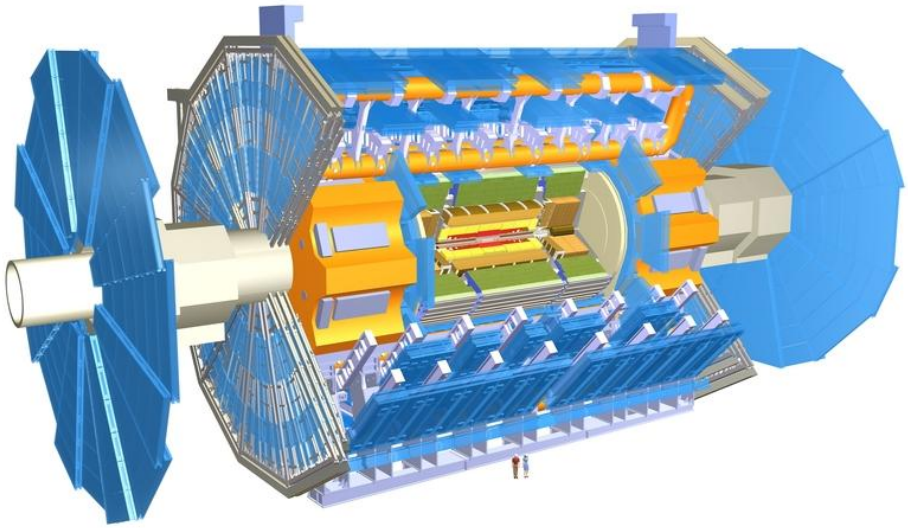

Figure 2: The ATLAS detector, weighing more than 7000 tons, consists of several concentric layers designed to identify and record the particles produced from LHC collisions. Credit: http://www-atlas.lbl.gov.

The ATLAS detector consists of three main sections [6]:

Inner Detector This innermost component tracks the motion of charged particles as they move away from the collision point. The 2 tesla magnetic field permeating the detector material deflects charged particles, whose direction of motion and degree of curvature become indicative of their

charge and momentum, respectively. The tracks measured in this section, by recording particle/detector interactions at a multitude of discrete points, form the first step in identifying the unknown particles.

Calorimeter The calorimeter measures the energy of both neutral and charged particles by interacting with them in such a way as to as to create a shower of secondary particles. This specific behaviour is achieved with a combination of spatially alternating absorbing and sensing elements, the former of which transform the primary particle into a cascade of secondary particles (known as a shower), and the latter of which quantifies the shower in such a way as to allow for the inference of the original particle's energy. The calorimeter is composed of two layers: the inner electromagnetic calorimeter, which interacts with photons, electrons/positrons etc., and the hadronic calorimeter, responsible for measuring the energy of its namesake particles.

Muon Spectrometer Muons are the only detectable particles capable of passing through the calorimeter without interaction. Thus, this outermost component, which functions in a similar manner as the inner detector, is used to measure the momentum of muons with high precision.

It is customary to use the coordinates η and ϕ to denote angular position with respect to the centre of the detector, where the collisions occur. Consider a spherical coordinate system set up at this central point, where ϕ is the azimuthal angle and θ is the polar angle. We define $\eta = -\ln[\tan(\theta/2)]$, a quantity known as pseudorapidity, as a replacement for the polar coordinate, as it is Lorentz invariant under boosts in the direction of the beam axis. Thus, $\eta = 0$ defines a plane through which the beam axis passes at a right angle, and $\eta = \pm\infty$ refer to the directions along the beam axis.

Finally, a distance in η-ϕ space is calculated as $\Delta R = \sqrt{\Delta\eta^2 + \Delta\phi^2}$, and is interpreted as a sort of solid angle from the centre of the detector.

3.2 Overall Trigger System

One of the main challenges faced by the ATLAS experiment is the need to reduce the data rate by selecting potentially interesting events for storage in real-time, so as to avoid being overwhelmed by the dominant QCD background processes [5].

Collisions occur in the ATLAS detector at the enormous rate of $\sim 10^9$ Hz. Not only is the DAQ system unable to record events at such a high rate, but if it could, we would soon end up with an unimaginably large amount of data. To deal with this problem, not only must the vast majority of the events be discarded, but it is imperative that interesting ones not be missed since they can be exceedingly rare (sometimes being produced at 10^{-13} times the interaction rate, or less) [2].

These challenges are addressed using the trigger system, which is composed of three levels, each of which reduces the rate of incoming data in succession. The three parts are known as the Level 1 (LVL1 or L1), Level 2 (LVL2 or L2), and the Event Filter (EF) triggers, the latter two of which are often referred to collectively as the High Level Trigger (HLT).

Level 1 This first level must deal with the highest input rate, and it is therefore based on custom hardware in order to make decisions as rapidly as possible. It uses coarse-granularity information from the calorimeter and the muon spectrometer to identify Regions of Interest (RoIs) in η-ϕ space, which get passed on to LVL2. Despite the fact that the Level 1 trigger is designed for speed, it cannot reach a decision in the $\sim$ 25 ns between bunch crossings, and so it stores information in pipelines for up to 2.5 μs while events are processed in parallel. When a decision is reached, an event is either rejected, or a list of RoIs is passed on to the Level 2 trigger [2]. The overall effect of LVL1 is to reduce the data rate from 40 MHz to 75 kHz [7].

Level 2 This is the first part of the High Level Trigger, and because of the reduced input rate from LVL1, it is based on software run on a computing farm, rather than on-site hardware. It is restricted to the RoIs identified by the Level 1 trigger, but uses full granularity data from all detectors in contrast to the aforementioned level. Nevertheless, this subset of the data represents only about 2% of the full event information, which allows the Level 2 trigger to reach relatively rapid decisions [2]. Events which pass this level are fully reconstructed and passed on to the Event Filter at a rate of 5.5 kHz [7].

Event Filter This second part of the High Level Trigger is also software based, and it represents the final level in the trigger system. Tasks involving greater computing complexity, such as bremsstrahlung recovery for electrons and conversion recovery for photons, are performed at this level. The data rate is reduced to 600 Hz before the events are finally recorded into mass storage [7].

3.3 The Trigger Menu

Thus far, events have been classified using the very broad labels of "interesting" and "not interesting". However, an experiment as complex as ATLAS obviously cannot use a one-size-fits-all trigger to make decisions, as there are a myriad of interesting event types. Thus, there is a list known as the trigger menu, and each individual trigger chain contained therein defines a set of criteria by which an event might be considered as "interesting", and selected for permanent storage.

The trigger chains in the menu are given names of the form *NzXX_i*, where the various components denote the following:

***N* (optional)** The minimum number of objects required.

z The type of selection, including

- e = electron
- g = photon (γ)
- E = total E_T, etc.

XX The minimum transverse energy required.

i An online quality requirement, such as *tight*, *loose* etc. This refers to one of many possible sets of criteria depending on the particle type, for example, the shape of the shower produced in the calorimeter.

Thus, the trigger chain *g20_loose* on which much of my work has been focused, is designed to accept *loose* (online) photons with $E_T > 20$ GeV.

Each chain is composed of LVL1, LVL2 and EF components. In the case of *g20_loose* these are *L1_EM12*, *L2_g20_loose* and *EF_g20_loose* respectively. Note that different trigger chains can share components; for example, *L1_EM12* is the LVL1 part of various electromagnetic chains.

Ordinarily, an event is recorded if it satisfies at least one trigger chain. However, a small fraction of events are recorded in "minimum bias" mode, meaning that they are selected for storage (almost) randomly, regardless of whether or not they satisfied any chain. Similarly, within a single chain, a certain fraction of events are "passed through" one or more components, meaning that they pass regardless of what the trigger's physics-based decision would have been. For example, an event might be satisfy *L1_EM12* and *L2_g20_loose*, and then be chosen at random to pass *EF_g20_loose* in passthrough mode. On the other hand, some events are rejected at random by a trigger chain, despite the fact that they meet the right criteria to pass. For example, if a chain would ordinarily select events at a rate which is too high for the DAQ system, it is often arranged that only 1 out of every n events be recorded, where n is known as the "prescale" factor.

3.4 Trigger Efficiency

In the case of a photon trigger chain such as *g20_loose*, the efficiency of the trigger, denoted ϵ, refers to the probability of a photon passing that particular chain. Efficiency is usually considered with respect to a kinematic variable, such as photon transverse energy, E_T^γ, which generates an efficiency curve, $\epsilon = \epsilon(E_T^\gamma)$. Ideally, *g20_loose* is designed to accept all online loose photons with $E_T > 20$ GeV and reject the rest, thus producing an efficiency curve shown in Fig. (3).

Conceptually, one could measure the efficiency of a photon trigger chain as follows: for a fixed range of photon E_T, the efficiency is simply the number of photons that passed the chain divided by the total number of photons in the

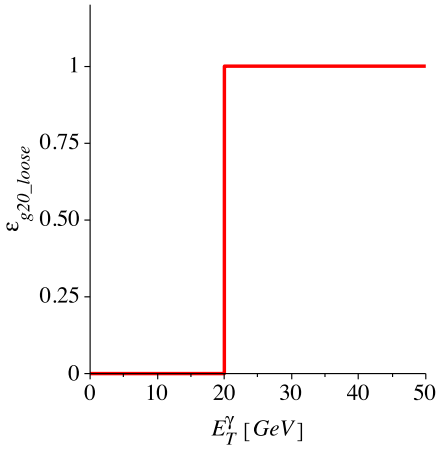

Figure 3: The idealized efficiency curve of *g20_loose*.

sample. One can repeat this for various bins of E_T^γ and construct a histogram representing the desired efficiency curve. To accomplish this, one would construct two histograms, the first containing the photons that passed the trigger chain, binned by E_T^γ, and the second containing all photons, with the same binning. Dividing the first histogram by the second would yield the desired efficiency curve. Unfortunately, this method is not realizable, as the total number of photons, *before* selection by the trigger, is unknown.

Fortunately, the existence of "minimum bias" events make studies such as this one possible. One could look at the photons contained in this minimum bias sample, split them into energy bins, and in each bin, calculate the fraction that *would have* passed *g20_loose*. However, the relatively small number of minimum bias events makes this approach unfeasible, as it would lead to overly large statistical uncertainties. In order to deal with this challenge, we employ the "bootstrap method".

4 Analysis

The measurement of inclusive photon production cross section requires one to know the efficiencies of the triggers which selected the photons used in the study. Thus, the criteria which define the set of photons considered in this trigger analysis are dictated by the photon cross section study. The efficiencies of the higher E_T photon triggers, which are also required to measure inclusive photon cross section, are measured with respect to ϵ_{g20_loose}, hence the focus on the *g20_loose* chain.

This analysis was conducted using ROOT, with scripts written in Python.

4.1 Offline Selection

We began our analysis by excluding events for which the `TTileTripReader` function in ROOT returned `True`. For each offline-identified photon in the remaining events, we defined a corrected energy, `ecor`, using the `EnergyRescalerUpgrade` tool in `egRescaler`, accounting for whether or not the photon was converted. We then defined photon transverse energy and momentum as $\texttt{ecor}/\cosh(\eta)$. Using the ROOT `PhotonIDTool`, we assigned to each photon a Boolean value, `isTight`, indicating whether or not it met offline *tight* requirements, based on the output of `PhotonCutsTight(tTight)`, where `tTight = 2012`. Finally, for each event, we considered only the leading tight photon, meaning the offline photon with `isTight = True` with the highest E_T^γ. If an event contained no tight photons at this stage, it was skipped altogether.

4.2 Bootstrap Method

As mentioned in § 3.4, statistical limitations, due to the size of the minimum bias sample, prevented us from computing the efficiency of the entire *g20_loose* chain as a single ratio.

For outcomes A and B belonging to a sample space Ω, the definition of conditional probability states that $P(A|B) = P(A \cap B)/P(B)$. Alternatively:

$$P(A \cap B) = P(A|B)P(B). \tag{3}$$

Recalling that a photon passing *g20_loose* is synonymous with it passing *L1_EM12* and the HLT portion of *g20_loose* (comprised of *L2_g20_loose* and *EF_g20_loose*), which I will refer to as *HLT_g20_loose*, we can use Eq. (3) to decompose the overall efficiency as

$$\epsilon_{g20\_loose} = \epsilon_{HLT\_g20\_loose\,|L1\_EM12} \;\times\; \epsilon_{L1\_EM12}. \tag{4}$$

I am using $\epsilon_{\alpha|\beta}$ to denote the efficiency of a trigger α with respect to events that have already passed the trigger β. Furthermore, to avoid overly cumbersome notation, I will leave the functional dependence of ϵ on E_T^γ implicit.

The advantage of decomposing ϵ_{g20_loose} as in Eq. (4), is that it allowed us to use different samples to calculate each term. To find ϵ_{L1_EM12}, we still had to use minimum bias events, although the requirement that an event pass *L1_EM12* is much less restrictive than requiring that it pass the entire *g20_loose* chain, thus greatly improving our statistics. For the efficiency of *HLT_g20_loose* with respect to *L1_EM12*, we no longer needed to use minimum bias events. Instead, we started with the full dataset and considered only events which passed *L1_EM12*, although in doing so we had to be careful to avoid biasing our sample.

Conceptually, to determine the efficiency of the HLT part of a chain with respect to the LVL1 component, we would divide the number of photons in a

given energy bin that passed the HLT and LVL1 by the number that passed LVL1. Again, we run into the problem that we don't have an accurate idea of the number which passed *only* LVL1. In order to resolve this problem, we limited ourselves to photons that were passed through *HLT_g20_loose*. This gave us an unbiased sample, from which we could ask what fraction *would have* passed the HLT based on physics requirements, in a given energy bin.

We can also further decompose our efficiency into LVL2 and EF efficiencies, rather than lumping them together as the HLT. For an additional outcome $C \subseteq \Omega$, Eq. (3) can be generalized as

$$P(A \cap B \cap C) = P(A|B)P(B|C)P(C), \tag{5}$$

which gives us the decomposition

$$\epsilon_{g20\_loose} = \epsilon_{EF\_g20\_loose\,|L2\_g20\_loose} \times \epsilon_{L2\_g20\_loose\,|L1\_EM12} \times \epsilon_{L1\_EM12}. \tag{6}$$

4.3 Trigger Decision Details

We used the `PyTrigDecisionToolD3PD` tool throughout our analysis to extract trigger information from event data. For a given event, one can call the Trigger Decision tool with the name of a trigger (e.g., *L1_EM12*) and a decision type (e.g., `Physics`, `PassedThrough` etc.), for which the tool returns a Boolean value, indicating whether or not an event passed the selected trigger in the specified mode. For example, the tool will return `True` for *L2_g20_loose* and `Physics` if the event in question passed the trigger because it satisfied the right physical requirements. Note that the decision types are not mutually exclusive, in that an event can, for example, return `True` for `Physics` and `passedThrough`, meaning that the event was passed through the trigger, but *would* have satisfied the right physical requirements.

The decision type `L1_TBP` provides the decision of LVL1 triggers *before* prescaling; a particularly convenient option, given that LVL1 triggers are often heavily prescaled. Unfortunately, there is no equivalent decision type provided for HLT triggers.

4.4 Histogram Criteria

In order to use Eq. (4) to decompose the efficiency, we measured the efficiency of the LVL1 triggers and the HLT (with respect to LVL1) separately. To do so, we made subsamples according to the criteria in Tables (1) and (2), binned the events contained therein by photon transverse energy, and divided the numerator histogram by the denominator.

We also further decomposed the *g20_loose* efficiency using Eq. (6), this time defining three subsamples according to Tables (1), (3) and (4). From these subsamples, we calculated the efficiency of each trigger component separately

	Trigger Requirement	Decision Type
Numerator	*EF_rd0_filled_NoAlg*	`Physics`
	L1_EM12	`L1_TBP`
Denominator	*EF_rd0_filled_NoAlg*	`Physics`

Table 1: LVL1 Histogram Criteria

	Trigger Requirement	Decision Type
Numerator	*L1_EM12*	`Physics`
	L2_g20_loose	`passedThrough`
	L2_g20_loose	`Physics`
	EF_g20_loose	`passedThrough`
	EF_g20_loose	`Physics`
Denominator	*L1_EM12*	`Physics`
	L2_g20_loose	`passedThrough`
	EF_g20_loose	`passedThrough`

Table 2: HLT Histogram Criteria

in the manner as described above, and multiplied the three resulting histograms together.

	Trigger Requirement	Decision Type
Numerator	*L1_EM12*	`Physics`
	L2_g20_loose	`passedThrough`
	L2_g20_loose	`Physics`
	EF_g20_loose	`passedThrough`
Denominator	*L1_EM12*	`Physics`
	L2_g20_loose	`passedThrough`
	EF_g20_loose	`passedThrough`

Table 3: LVL2 Histogram Criteria

	Trigger Requirement	Decision Type
Numerator	*L1_EM12*	`Physics`
	L2_g20_loose	`Physics`
	EF_g20_loose	`passedThrough`
	EF_g20_loose	`Physics`
Denominator	*L1_EM12*	`Physics`
	L2_g20_loose	`Physics`
	EF_g20_loose	`passedThrough`

Table 4: EF Histogram Criteria

In the early stages of this analysis, we repeatedly measured an HLT efficiency

turn-on curve that plateaued at 0.5 instead of at 1. Further examination revealed that the issue was with the EF efficiency, with respect to photons having passed LVL2. We found that by only considering events which were recorded without an EF prescale, we recovered the expected efficiency. This selection didn't have a major impact on the quality of our statistics, so we kept it throughout the rest of the analysis.

4.5 Propagation of Uncertainty

The efficiency in each bin effectively follows a binomial distribution. In order to get the proper uncertainties, we calculate the Clopper-Pearson interval associated with every bin using the `Divide` function in the `TGraphAsymmErrors` ROOT class. We performed this procedure for LVL1 and HLT histograms separately (or LVL1, LVL2 and EF separately, when using Eq. (6)) and multiplied the resulting efficiency histograms together to obtain the full chain efficiency.

Even in the approximation where the two (or three) efficiency histograms are independent, there is no straightforward way to multiply Clopper-Pearson intervals. As an ad-hoc substitute, we use the following relation, which gives the variance of the product of two random variables X and Y [8]:

$$\mathrm{Var}(XY) = E(X)^2\,\mathrm{Var}(Y) + E(Y)^2\,\mathrm{Var}(X) + \mathrm{Var}(X)\,\mathrm{Var}(Y). \qquad (7)$$

Treating the upper and lower errors in each bin separately as pseudo standard deviations, we approximated the uncertainty in the overall efficiency. Thankfully, for the purposes of the inclusive photon production study, the efficiencies of the HLT and LVL1 portions of *g20_loose* are more useful when considered separately, so knowing the exact confidence intervals on the total efficiency is not essential.

5 Results

Using the criteria defined in § 4.4, we created numerator and denominator histograms for *L1_EM12* and *HLT_g20_loose* (with respect to *L1_EM12*) and divided them to get the LVL1 and HLT efficiencies of the *g20_loose* trigger chain, shown in Fig. (4).

We performed a similar procedure using Eq. (6) and considered *L2_g20_loose* and *EF_g20_loose* separately. The efficiencies resulting from this approach are shown in Fig. (5).

Using either approach, the resulting efficiencies can be multiplied together to yield the full *g20_loose* efficiency, as shown in Fig. (6). Note that both methods gave the same results (including uncertainties), as this fact represents an important crosscheck.

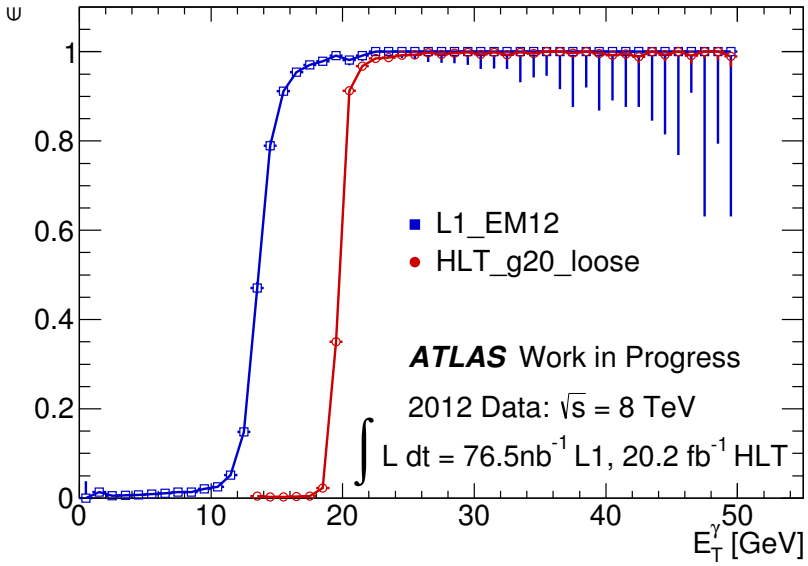

Figure 4: $\epsilon_{HLT\_g20\_loose|L1\_EM12}$ & ϵ_{L1_EM12} vs. E_T^γ

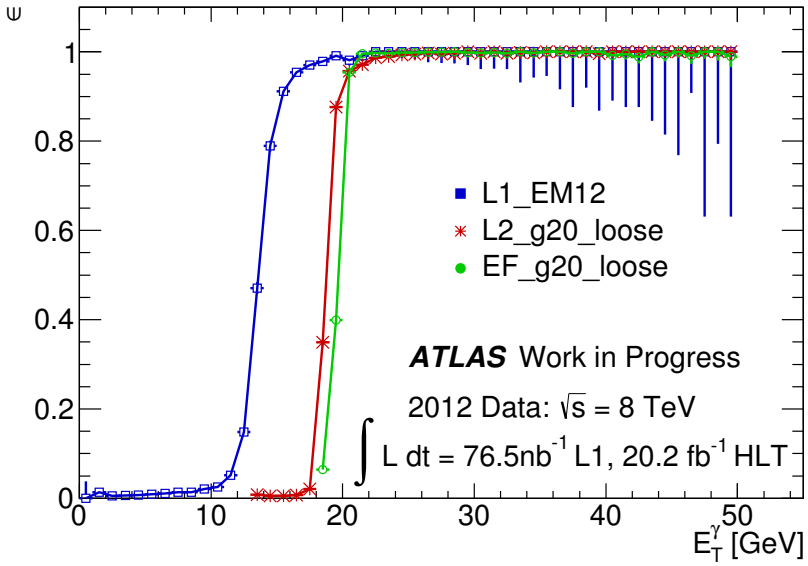

Figure 5: $\epsilon_{EF\_g20\_loose|L2\_g20\_loose}$, $\epsilon_{L2\_g20\_loose|L1\_EM12}$ & ϵ_{L1_EM12} vs. E_T^γ

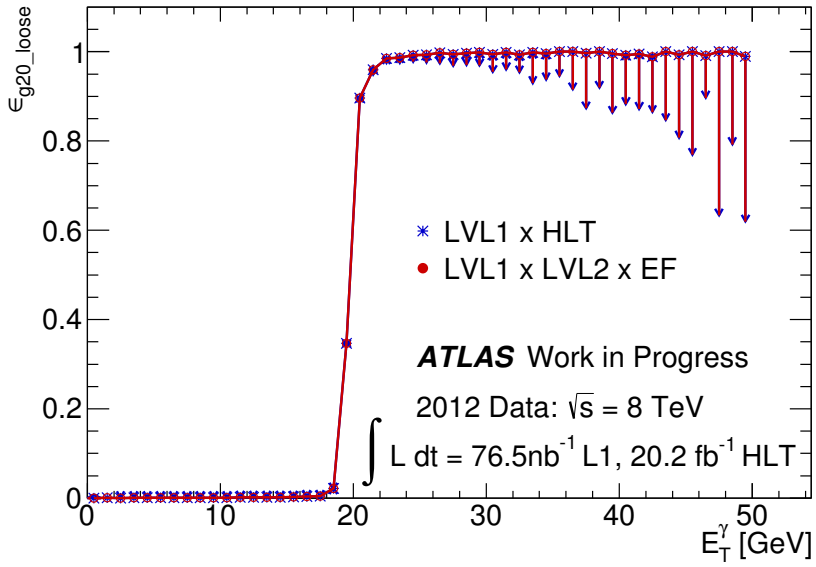

Figure 6: ϵ_{g20_loose} vs. E_T^γ measured in two different ways.

Upon examination of the efficiency turn-on curves in Fig. (6) (and Table (5) in the Appendix), one finds that the ϵ_{g20_loose} reaches a plateau near 100% at $E_T^\gamma = 23$ GeV.

6 Conclusions

Despite our use of the bootstrap method, the lower uncertainties in the high-E_T^γ region remain rather large. The limiting factor here seems to be in the *L1_EM12* efficiency, due to the limited number of minimum bias events, and the falling transverse energy spectrum of leading photons.

Nevertheless, the measured efficiency of *g20_loose* reaches a plateau above $E_T^\gamma = 23$ GeV, wherein it remains consistent with full efficiency to within $\sim 1\%$. The results do not differ depending on the bootstrap decomposition used (i.e., Eq. (4) or Eq. (6)).

The next step of the inclusive photon cross section analysis involves using a sort of bootstrap method to determine the efficiency of higher E_T-cutoff photon triggers, based on ϵ_{g20_loose}. If the uncertainties in the latter efficiency prove to be a limiting factor, we may complement this study with a radiative Z-decay analysis.

References

[1] CERN, *The Standard Model*, 2013. `http://home.web.cern.ch/about/physics/standard-model`.

[2] R. Hauser, *The ATLAS trigger system*, Eur. Phys. J. **C34** (2004) S173–S183.

[3] ATLAS Collaboration, *Measurement of the inclusive isolated prompt photon cross section in pp collisions at* $\sqrt{s} = 7$ *TeV with the ATLAS detector*, Phys. Rev. D **83** (2011) 052005.

[4] J. Pivarski, "Cross section." Fermilab Today, March 1, 2013.

[5] J. Alison et al., *Performance of the ATLAS Electron and Photon Trigger in p-p Collision at* $\sqrt{s} = 7$ *TeV in 2011*, ATLAS-CONF-2012-048 (2012).

[6] ATLAS, "Detector Description." `http://www.atlas.ch/detector.html`.

[7] ATLAS Collaboration, *The ATLAS Experiment at the CERN Large Hadron Collider*, Journal of Instrumentation **3** no. 08, (2008) S08003.

[8] L. A. Goodman, *On the Exact Variance of Products*, Journal of the American Statistical Association **55** no. 292, (1960) 708–713.

[9] B. Dahmes, *Triggers for LHC Physics*, in *CERN Summer Student Lectures*. 2013.

[10] L. Yuan, "Recent g20_loose trigger efficiency measure study." Presentation Slides, 2009.

[11] V. Chiochia, G. Dissertori, and T. Gehrmann, "Particle Physics Phenomenology 1." Course Notes, 2010.

[12] ATLAS Collaboration, *Measurement of isolated-photon pair production in pp collisions at* $\sqrt{s} = 7$ *TeV with the ATLAS detector*, JHEP **1301** (2013) 086.

Appendix

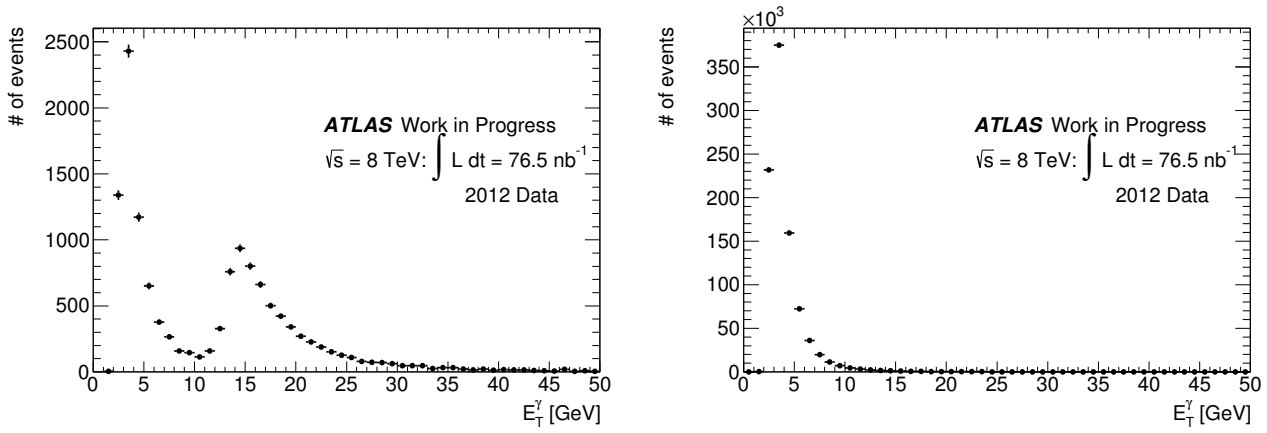

(a) Numerator (b) Denominator

Figure 7: Histograms used to compute the efficiency of *L1_EM12*.

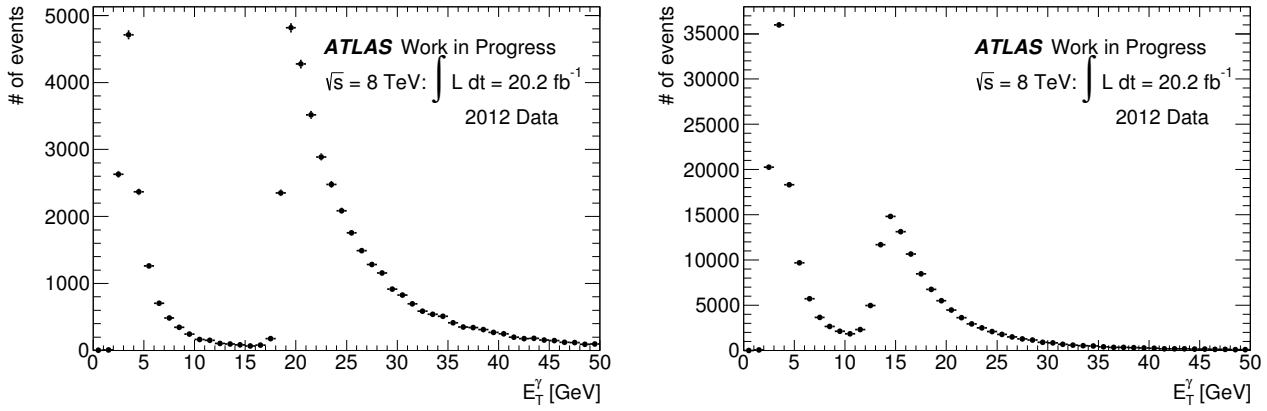

(a) Numerator (b) Denominator

Figure 8: Histograms used to compute the efficiency of *L2_g20_loose* with respect to *L1_EM12*.

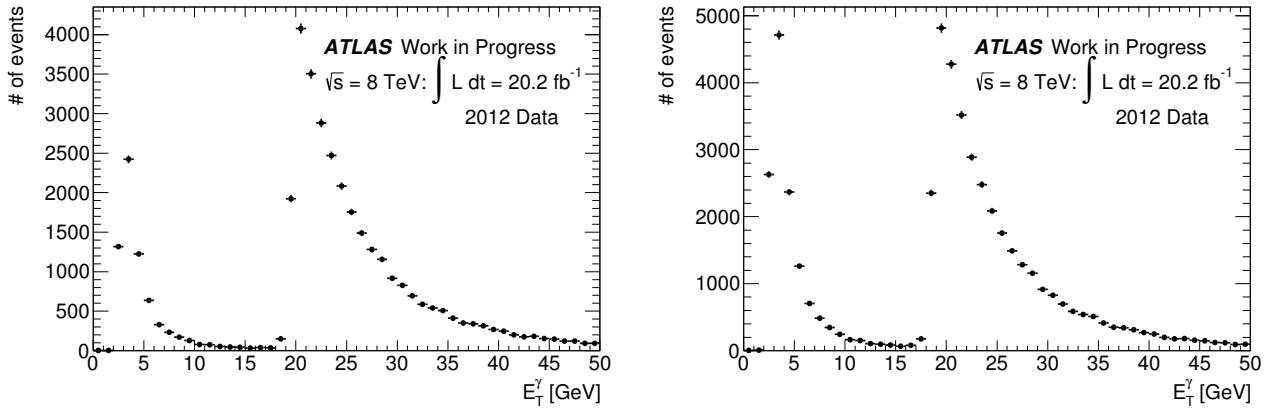

(a) Numerator

(b) Denominator

Figure 9: Histograms used to compute the efficiency of *EF_g20_loose* with respect to *L2_g20_loose*.

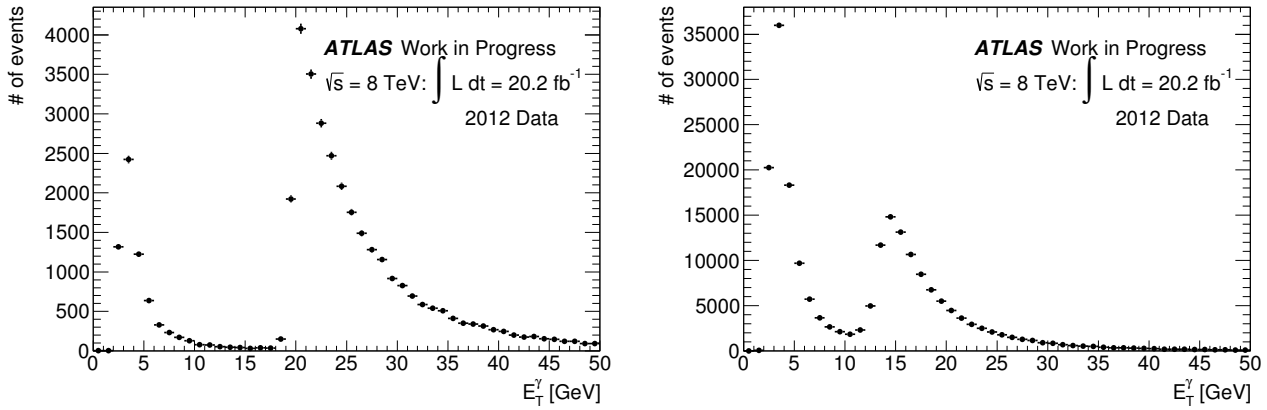

(a) Numerator

(b) Denominator

Figure 10: Histograms used to compute the efficiency of *HLT_g20_loose* with respect to *L1_EM12*.

Bin #	Lower Bound	Measured	Upper Bound
1	0.0	0.0	0.00225031392031
2	0.00082870960993	0.000853630776235	0.000879187400164
3	0.000364394530967	0.000375842302204	0.000387512634197
4	0.000417365461443	0.000436107694364	0.00045537397233
5	0.000461483287485	0.000491427575789	0.000522516777099
6	0.000546570663233	0.000591593812469	0.000638951531328
7	0.000542122100388	0.000605907382115	0.000673628211911
8	0.000762332985102	0.0008574766226	0.000959904381299
9	0.000769060351044	0.000899979704855	0.00104188509769
10	0.00106539638021	0.00123755360657	0.00142696067828
11	0.000897420180367	0.00109470665737	0.00130888908744
12	0.00139527686237	0.00165123307788	0.00192062447732
13	0.00142327025802	0.00158512987025	0.00175506027569
14	0.0017272707018	0.00193650669119	0.00217854247483
15	0.00184668874136	0.00218572711536	0.00258943995765
16	0.00168104881002	0.00221937815331	0.00284911586195
17	0.00289870001028	0.00358058303287	0.00438287146261
18	0.00249007375231	0.00424161735925	0.00613610353707
19	0.01556594629	0.0219281422254	0.0283424496992
20	0.340782176922	0.346884687461	0.351901493531
21	0.885310987831	0.896137024756	0.902009050397
22	0.950070427298	0.959803933347	0.962029693811
23	0.972737960296	0.98496754356	0.987206810765
24	0.972799721302	0.987210231815	0.98909174385
25	0.975559380813	0.992377322535	0.994306798763
26	0.970233312208	0.993208828523	0.994489752406
27	0.971961422176	0.997322623829	0.999464215329
28	0.968220131058	0.993803253292	0.995454258775
29	0.967285012664	0.996548748921	0.997450889044
30	0.960325027216	0.998909487459	1.0
31	0.9564429644	0.993990384615	0.995178987573
32	0.959836172407	0.998563218391	1.0
33	0.925192301632	0.993220338983	0.99474386329
34	0.940377000168	0.998158379374	1.0
35	0.941860691097	0.99609375	0.99609375
36	0.915902150783	1.0	1.0
37	0.87659145381	1.0	1.0
38	0.916803301522	0.997058823529	0.997058823529
39	0.867677813818	1.0	1.0
40	0.887494684943	0.996296296296	1.0
41	0.869196741114	0.991967871486	0.996104475532
42	0.871511461494	0.995	1.0
43	0.836042272439	0.988764044944	0.988764044944
44	0.814413809948	1.0	1.0
45	0.763452044509	0.99358974359	0.99358974359
46	0.905781379846	1.0	1.0
47	0.625589582385	0.991803278689	0.991803278689
48	0.793480757268	1.0	1.0
49	0.630252089077	1.0	1.0

Table 5: Measured efficiency of *g20_loose* obtained by multiplying LVL1 and HLT efficiencies.